

Ambient Temperature Plastic Crystal Electrolyte for Efficient, All-Solid-State Dye-Sensitized Solar Cell

Peng Wang,[†] Qing Dai,^{*,‡} Shaik M. Zakeeruddin,[†] Maria Forsyth,[‡] Douglas R. MacFarlane,[‡] and Michael Grätzel^{*,†}

Laboratory for Photonics and Interfaces, Swiss Federal Institute of Technology, CH 1015, Lausanne, Switzerland, and School of Chemistry, Monash University, Willington Road, Clayton, Victoria 3800, Australia

Received August 18, 2004; E-mail: michael.graetzel@epfl.ch

In the past decade, considerable scientific and industrial research efforts have been devoted to the nanocrystalline dye-sensitized solar cell (DSC) since its first successful demonstration in 1991.¹ This type of inorganic–organic hybrid device has been widely considered as a potential, low-cost alternative to the conventional inorganic photovoltaic cells due to its ability to achieve an efficiency better than 10%.² Recent achievements in the long-term stability under the thermal and light-soaking stress have further enhanced its commercial prospect.³ While further improvements in power conversion efficiency are sought by designing more efficient sensitizers and electron mediators, fabricating better nanostructured semiconductor films, and more deeply understanding the interfacial charge-transfer process, replacing the volatile organic solvent normally employed in high efficiency devices is also highly desirable in view of the practical issue of long-term robust encapsulation. In this context, solvent-free ionic liquid electrolytes have been pursued, and very recently, considerably high device efficiencies of 7–8.3% were achieved.⁴ On the other hand, p-type inorganic semiconductors,⁵ organic hole-transport materials,⁶ and solvent-free polymer electrolytes,⁷ incorporating the triiodide/iodide redox couple, were investigated for solid-state dye-sensitized solar cells; however, all of these types of devices have yet to reach a 5% efficiency.

Plastic crystals are compounds where the molecules or ions exhibit rotational disorder, while their centers of mass occupy ordered sites in the crystalline lattice structure.⁸ These rotator phases usually occur via solid–solid transitions below the melting point, and often produce plastic properties and good mechanical flexibility, as well as relatively high conductivity of either doped ions or matrix ions in the case of ionic plastic crystal compounds. Recently, considerable interest in plastic crystals has been revived after the recognition of their potential function as a new type of solid electrolyte in lithium batteries and fuel cells.⁹

Succinonitrile is a well-known example of a molecular plastic crystal-forming compound. It forms a monoclinic structure at low temperatures, which undergoes a first-order transition to a plastic phase at -40 °C. The plastic phase of succinonitrile then occupies a body-centered cubic structure until it melts at 58 °C. In this phase, the molecules exist in three isomeric conformations (two gauche isomers and one trans isomer), which are interrelated by a 120° rotation around the central C–C bond.¹⁰ Molecular dynamics studies¹¹ have shown that the disorder in the plastic phase is related to the trans–gauche isomerization (involving a rotation about the central C–C bond) of the molecules and molecular jumps from one diagonal position of the cubic structure to another. Hawthorne and Sherwood¹² have suggested that the availability of three possible conformers in succinonitrile has a major effect on the diffusion

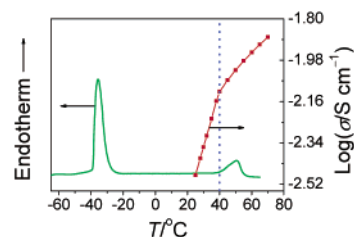


Figure 1. Differential scanning calorimetric trace and the conductivity–temperature plot for the $P_{1,4}I$ -doped solid electrolyte.

capacity of the molecules, where the trans isomers act as “impurities” and create monovacancies in the lattice, hence, leading to the high molecular diffusivity. Interestingly, doping this solid-state matter with solid acids, such as lithium and other metal salts, has resulted in good fast ion conductors over a wide temperature range.^{9e–h} Here, we report the conductivity, diffusion, and photovoltaic data for a *N*-methyl-*N*-butylpyrrolidinium iodide¹³ ($P_{1,4}I$)-doped succinonitrile plastic crystal electrolyte. For the first time, efficiencies exceeding 6.5% have been achieved in an all-solid-state dye-sensitized solar cell.

The plastic crystal electrolyte was made by mixing $P_{1,4}I$, I_2 , and succinonitrile in a mole ratio of 5:1:100, and the mixture was then heated to ~ 70 °C. After the mixture was cooled to room temperature, a waxy solid was obtained. Here, succinonitrile functions as the solid solvent for the doped ions. As a portion of the iodide reacts with the iodine to form triiodide, the iodide and triiodide concentrations in this solid electrolyte were calculated to be approximately 0.49 and 0.12 M, respectively. Differential scanning calorimetric scans were obtained to investigate the phase behavior of the plastic crystal electrolyte. As shown in Figure 1, the plastic crystal phase was observed between -40 and 40 °C. Doping with $P_{1,4}I$ and iodine decreases the melting point from 58 to 50 °C, while the normal crystal to plastic crystal transition temperature remained unaffected. The conductivity–temperature plot in Figure 1 shows that the material is highly conductive in its plastic phase. At 25 °C, the plastic crystal electrolyte has a conductivity of 3.3 mS/cm, which is even higher than that (< 1 mS/cm) for the 1-propyl-3-methylimidazolium iodide-based ionic liquid electrolyte.¹⁴

A two-electrode electrochemical cell, with a Pt ultramicroelectrode (radius = 5 μm) as the working electrode and a Pt foil as the counter electrode, described in our previous work,¹⁴ was employed for diffusion coefficient determination. The steady-state voltammogram of the material, showing the iodide/triiodide redox processes, is presented in Figure 2. The apparent diffusion coefficients (D_{app}) of iodide and triiodide can be calculated from the anodic and cathodic steady-state currents (I_{ss}) according to the equation, $I_{\text{ss}} = 4ncaFD_{\text{app}}$, where n is the electron-transfer number per species. F is the Faraday constant; a is the radius of the

[†] Swiss Federal Institute of Technology.

[‡] Monash University.

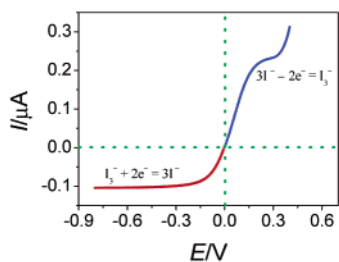


Figure 2. Steady-state voltammogram of a Pt ultramicroelectrode in the molecular plastic crystal electrolyte (scan rate = 10 mV/s).

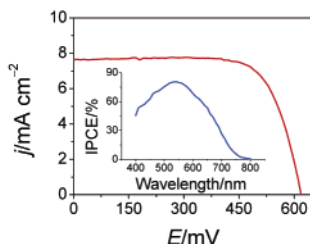


Figure 3. J - V curve of devices with the $P_{1,4}I$ -doped molecular plastic crystal electrolyte under illumination at 51.9 mW/cm². The inset is the photocurrent action spectrum. Cell area tested with mask (0.158 cm²).

ultramicroelectrode, and c is the bulk concentration of the electroactive species.¹⁵ The diffusion coefficients of iodide and triiodide in this solid electrolyte at room temperature were determined to be 3.7×10^{-6} and 2.2×10^{-6} cm²/s, respectively, which is higher than those in the solvent-free ionic liquid electrolytes.^{4b,14} The observed fast ion transport in this solid material can be seen as a decoupling of diffusion and shear relaxation times, which probably originates from local defect rotations in the succinonitrile plastic crystal.

A screen-printed double layer of TiO₂ particles was used as the photoanode. An 8- μ m-thick film of 20-nm-sized TiO₂ particles was first printed on the fluorine-doped SnO₂ conducting glass electrode and further coated by a 5- μ m-thick second layer of 400-nm-sized light-scattering anatase particles. Detailed fabrication procedures for the nanocrystalline TiO₂ photoanodes have been described elsewhere.¹⁶ The TiO₂ electrodes were immersed at room temperature for 12 h into a solution containing 300 μ M N-719 dye¹⁷ in acetonitrile and *tert*-butyl alcohol (1:1, v/v). The electrodes and platinized conducting glass were separated by a 25- μ m-thick Surlyn hot-melt ring (DuPont) and sealed up by heating. The above-mentioned solid electrolyte was heated until it became a liquid and injected into the warmed sandwiched cells using a vacuum back-filling system. After the solution was cooled to room temperature, a uniform solid electrolyte was formed in the cells. The electrolyte-injecting hole made with a sand-blasting drill on the counter electrode glass substrate was sealed with a Surlyn sheet and a thin glass cover by heating.

The photocurrent action spectrum of the solid DSC is presented in the inset of Figure 3. The incident photon to current conversion efficiency (IPCE) exceeds 60% in a broad spectral range from 440 to 630 nm, reaching its maximum of about 80% at 540 nm. As shown in Figure 3, the short-circuit photocurrent density (J_{sc}), the open-circuit photovoltage (V_{oc}), and the fill factor (ff) of nanocrystalline dye-sensitized solar cells, with the $P_{1,4}I$ -doped molecular plastic crystal electrolyte under the illumination by 51.9 mW/cm² sunlight (AM 1.5), are 7.8 mA/cm², 618 mV, and 0.735, respectively, yielding an overall conversion efficiency (η) of 6.7%. At various lower incident light intensities, overall power conversion efficiencies are also >6.5%. Under full sunlight, the efficiency

dropped to ~5%, probably due to the inefficient charge screening of electron transport in the nanocrystalline film. This is the first time such a high efficiency has been reached by an all-solid-state dye-sensitized solar cell. At this stage, we are still optimizing the composition of the plastic crystal electrolytes by varying the cations to reach optimal photovoltaic performance. This study also will address the problem of the photocurrent decrease that we noted during preliminary stability tests with the current electrolyte composition.

In summary, we have demonstrated that doping the molecular plastic crystal with a solid iodide salt and iodine has produced a highly conductive solid iodide/triiodide conductor. It was further employed in a regenerative dye-sensitized solar cell yielding an unprecedented power conversion efficiency of 6.7% under AM 1.5 radiation (51.9 mW/cm²) for solid organic photovoltaic devices. We believe this concept may also be explored for other solid electrolytes in dye-sensitized solar cells by doping other electron mediators in various plastic crystal materials.

Acknowledgment. The present work is supported by the Swiss Science Foundation, the Swiss Federal Office for Energy (OFEN), and the European Office of the U.S. Air Force, under Contract F61775-00-C0003. Q.D. thanks the Australia Research Council for financial support.

References

- (1) (a) O'Regan, B.; Grätzel, M. *Nature* **1991**, *353*, 737. (b) Grätzel, M. *Nature* **2001**, *414*, 338.
- (2) Grätzel, M. *J. Photochem. Photobiol., A* **2004**, *164*, 3.
- (3) (a) Wang, P.; Zakeeruddin, S. M.; Moser, J. E.; Nazeeruddin, M. K.; Sekiguchi, T.; Grätzel, M. *Nat. Mater.* **2003**, *2*, 402. (b) Wang, P.; Zakeeruddin, S. M.; Humphry-Baker, R.; Moser, J. E.; Grätzel, M. *Adv. Mater.* **2003**, *15*, 2101.
- (4) (a) Wang, P.; Zakeeruddin, S. M.; Moser, J. E.; Humphry-Baker, R.; Grätzel, M. *J. Am. Chem. Soc.* **2004**, *126*, 7164. (b) Wang, P.; Zakeeruddin, S. M.; Humphry-Baker, R.; Grätzel, M. *Chem. Mater.* **2004**, *16*, 2694.
- (5) (a) Kumara, G. R. A.; Kaneko, S.; Okuya, M.; Tennakone, K. *Langmuir* **2002**, *18*, 10493. (b) O'Regan, B.; Lenzenmann, F.; Muis, R.; Wienke, J. *Chem. Mater.* **2002**, *14*, 5023.
- (6) (a) Krüger, J.; Plass, R.; Grätzel, M.; Matthieu, H.-J. *Appl. Phys. Lett.* **2002**, *81*, 367. (b) Kitamura, T.; Maitani, M.; Matsuda, M.; Wada, Y.; Yanagida, S. *Chem. Lett.* **2001**, 1054.
- (7) (a) Nogueira, A. F.; Durrant, J. R.; De Paoli, M. A. *Adv. Mater.* **2001**, *13*, 826. (b) Stergiopoulos, T.; Arabatzis, I. M.; Katsaros, G.; Falaras, P. *Nano. Lett.* **2002**, *2*, 1259.
- (8) (a) Timmermans, J. *J. Phys. Chem. Solids* **1961**, *18*, 1. (b) Smith, G. W. *Int. Sci. Technol.* **1967**, *61*, 72. (c) Angell, C. A. *J. Non-Cryst. Solids* **1991**, *131-133*, 13. (d) Smith, G. W. *Comments Solid State Phys.* **1978**, *9*, 21.
- (9) (a) MacFarlane, D. R.; Huang, J.; Forsyth, M. *Nature* **1999**, *402*, 792. (b) Forsyth, M.; Huang, J.; MacFarlane, D. R. *J. Mater. Chem.* **2000**, *10*, 2259. (c) Alarco, P.-J.; Abu-Lebdeh, Y.; Armand, M. *Angew. Chem., Int. Ed.* **2003**, *42*, 4499. (d) Alarco, P.-J.; Abu-Lebdeh, Y.; Ravet, N.; Armand, M. *Solid State Ionics* **2004**, in press. (e) Long, S.; MacFarlane, D. R.; Forsyth, M. *Solid State Ionics* **2003**, *161*, 105. (f) Abu-Lebdeh, Y.; Abouimrane, A.; Alarco, P.-J.; Hammami, A.; Ionescu-Vasii, L.; Armand, M. *Electrochem. Commun.* **2004**, *6*, 432. (g) Alarco, P.-J.; Abu-Lebdeh, Y.; Abouimrane, A.; Armand, M. *Nat. Mater.* **2004**, *3*, 476. (h) Abouimrane, A.; Abu-Lebdeh, Y.; Alarco, P.-J.; Armand, M. *J. Electrochem. Soc.* **2004**, *151*, A1028.
- (10) (a) Bischofberger, T.; Courtens, E. *Phys. Rev. Lett.* **1974**, *32*, 163. (b) Derollez, P.; Lefebvre, J.; Descamps, M.; Press, W.; Fontaine, H. *J. Phys.: Condens. Matter* **1990**, *2*, 6893.
- (11) Gardini, G.; Righini, R.; Califano, S. *J. Chem. Phys.* **1991**, *95*, 679.
- (12) Hawthorne, H. M.; Sherwood, J. N. *Trans. Faraday Soc.* **1970**, *66*, 1792.
- (13) MacFarlane, D. R.; Meakin, P.; Sun, J.; Amini, N.; Forsyth, M. *J. Phys. Chem. B* **1999**, *103*, 4164.
- (14) Wang, P.; Zakeeruddin, S. M.; Comte, P.; Exnar, I.; Grätzel, M. *J. Am. Chem. Soc.* **2003**, *125*, 1166.
- (15) Bard, A. J.; Faulkner, L. R. *Electrochemical Methods: Fundamentals and Applications*, 2nd ed; Wiley: Weinheim, Germany, 2001.
- (16) Wang, P.; Zakeeruddin, S. M.; Comte, P.; Charvet, R.; Humphry-Baker, R.; Grätzel, M. *J. Phys. Chem. B* **2003**, *107*, 14336.
- (17) Nazeeruddin, M. K.; Kay, A.; Rodicio, I.; Humphry-Baker, R.; Müller, E.; Liska, P.; Vlachopoulos, N.; Grätzel, M. *J. Am. Chem. Soc.* **1993**, *115*, 6382.

JA045013H